Numerical Simulation and Analysis of Swirling Flow in the Draft Tube Cone of a Francis Turbine

Romeo SUSAN-RESIGA "Politehnica" University of Timişoara, Romania
resiga@mh.mec.upt.ro
Gabriel Dan CIOCAN École Polytechnique Fédérale de Lausanne, Switzerland
GabrielDan.Ciocan@epfl.ch
Sebastian MUNTEAN Romanian Academy-Timişoara Branch, Romania
seby@acad-tim.tm.edu.ro
Ioan ANTON "Politehnica" University of Timişoara, Romania
anton@acad-tim.tm.edu.ro
François AVELLAN École Polytechnique Fédérale de Lausanne, Switzerland
Francois.Avellan@epfl.ch

Key words: Decelerated swirling flow, draft tube cone, flow control.

Abstract

The paper presents numerical investigations of decelerated swirling flows specific to hydraulic turbines draft tube cone, within the framework of axisymmetric flow models. First, we investigate the behaviour of a Burgers vortex in a diffuser as the swirl intensity is increased. We show that first a steady vortex breakdown occurs, with a central stagnation region, then the flow becomes highly unsteady with vortex rings convected downstream. Our main result proves that the vortex breakdown and the unsteadiness can be removed by slighlty altering the inlet axial velocity profile. A rather weak water jet injected at the axis in the inlet section, recovers a steady breakdown-free flow configuration. Second, we validate and assess the accuracy of the turbulent axisymmetric flow model in comparison with velocity and turbulent kinetic energy measurements in a model Francis turbine draft tube cone.

Introduction

Axisymmetric flow models are the main tool for preliminary design and analysis of turbomachinery swirling flows. The resulting quasi-three-dimensional (Q3D) methodologies are now widely used in conjunction with a swirl schedule in the bladed regions to design the rotating and non-rotating blades (Ref 1). However, the steady axisymmetric swirling flow assumption, which reduces the Euler equations to a single non-linear equation (known in literature as Long-Squire or Bragg-Hawthorne equation), may fail when the swirling flow

downstream the turbine runner is decelerated in the draft tube cone. Even if the flow remains practically steady and axisymmetric in the cone, the occurrence of vortex breakdown calls for special techniques to capture the central quasi-stagnation region that develops in these cases. Keller et al. (Ref 2) show that the loss-free, incompressible, steady axisymmetric model described by the Long-Squire equation can provide solutions for decelerated swirling flows up to a certain swirl number. If the swirl intensity is further increased there is no steady solution, and time-dependent axi-symmetric or full 3D flow models must be used. However, the relative low computational cost associated with the axial-symmetry hypothesis has motivated further developments with relevant practical results.

A fruitful approach is to investigate the stability properties of steady axisymmetric flow configurations. Starting with the Benjamin's paper (Ref 3), the past four decades have witnessed numerous developments particularly within the framework of vortex breakdown studies. Our recent results (Ref 4) identified the transition from supercritical to subcritical state of the swirling flow ingested by a Francis turbine draft tube as the cause of a peculiar jump in the draft tube pressure recovery coefficient in the neighborhood of the best efficiency operating point. Zhang et al. (Ref 5) investigate the origin of severe pressure fluctuations in Francis hydraulic turbines at off-design conditions from hydrodynamic stability viewpoint. They build an axisymmetric steady swirling flow for three operating regimes by temporal-azimuthal averaging full 3D unsteady flow simulations. Then, these base flows are approximated on several cross-sections, and a stability analysis is conducted. Their main result shows that at the best efficiency point the whole flow is convectively unstable, meaning that any perturbation is convected downstream. However, as the discharge decreases the swirling flow becomes absolutely unstable starting from a certain station. When the fully developed vortex rope is observed at partial discharge, the averaged axi-symmetric swirling flow is absolutely unstable from the inlet section of the cone. A similar technique is employed by Gallaire et al. (Ref 6) who demonstrate that the non-axisymmetric spiral vortex breakdown states observed at moderate Reynolds numbers may be interpreted as resulting from a global instability of the axisymmetric vortex breakdown state. All these theoretical considerations rely on a steady axi-symmetric flow configuration which may be obtained either by circumferentially averaging experimental data, by using an inviscid or viscous axisymmetric flow solver (Ref 7), or simply by imposing various inlet swirl configurations such as a rigid body rotation, a Rankine, Burgers or Bachelor vortex, or a combination of these basic swirling flows.

The present paper is focused on using axisymmetric flow models to investigate decelerated swirling flows specific to the hydraulic turbines draft tube cones. Instead of investigating the flow stability, we ask ourselves the fundamental question: *Is there any hydrodynamic mechanism to mitigate the unsteadiness at high swirl numbers*? First, we investigate the evolution of a Burgers vortex in a diffuser as the swirl intensity is increased. Using an unsteady axi-symmetric Euler solver, we show that a steady swirling flow develops a vortex breakdown with a central stagnation core, according to Keller et al. (Ref 2), and then it becomes highly unsteady as the swirl intensity increases. *The main result of this investigation*

is that the unsteady swirling flow can be stabilized to a steady configuration by injecting a central jet on the inlet section. Although this jet has only 0.5% of the overall discharge and a velocity only 50% larger than the averaged inlet discharge velocity, it manages to remove all flow field fluctuations. This result is particularly relevant for Francis turbines operating at part load, where the unsteady helical vortex breakdown in the draft tube cone, also known as "vortex rope", leads to severe pressure fluctuations with associated safety risks. In comparison with classical air admission, conical extensions of the runner crown, stabilizing fins on the cone wall, and other practical solutions, the flow control technique that uses a water jet injected at the crown cone tip is aimed directly at mitigating the primary source of unsteadiness, namely the vortex rope. Moreover, since the unsteady vortical flow structures, that capture a significant fraction of kinetic energy and then dissipate it through viscous mechanisms, are eliminated we expect a significant reduction in hydraulic losses with the associated improvement in the draft tube efficiency. The last part of the paper is devoted to validation and accuracy assessment of the axisymmetric turbulent flow solver with experimental data from the FLINDT project (Ref 8).

Axisymmetric inviscid flow simulation and swirling flow control

Axisymmetric flow of inviscid incompressible fluids is governed by the Euler equations in cylindrical coordinates (z, r, θ),

$$\frac{\partial V_z}{\partial z}+\frac{\partial V_r}{\partial r}+\frac{V_r}{r}=0\text{, continuity,} \tag{1}$$

$$\frac{\partial V_z}{\partial t}+V_z\frac{\partial V_z}{\partial z}+V_r\frac{\partial V_z}{\partial r}=-\frac{1}{\rho}\frac{\partial p}{\partial z}\text{, axial momentum,} \tag{2}$$

$$\frac{\partial V_r}{\partial t}+V_z\frac{\partial V_r}{\partial z}+V_r\frac{\partial V_r}{\partial r}-\frac{V_\theta^2}{r}=-\frac{1}{\rho}\frac{\partial p}{\partial r}\text{, radial momentum,} \tag{3}$$

$$\frac{\partial V_\theta}{\partial t}+V_z\frac{\partial V_\theta}{\partial z}+V_r\frac{\partial V_\theta}{\partial r}+\frac{V_rV_\theta}{r}=0\text{, tangential momentum,} \tag{4}$$

where V_z, V_r, and V_θ are the axial, radial and swirl velocity components, p is the pressure and ρ the density. The axisymmetric Euler solver from the FLUENT 6.2.16 code is used for the numerical investigations further presented in this section.

The computational domain corresponds to the diffuser shape considered by Keller et al. (Ref 2), with the wall radius given by

$$\frac{r_{\text{wall}}(z)}{R_{\text{in}}}=1+\frac{1}{2}\left[1-\cos\left(\pi\frac{z}{6}\right)\right]\ \text{for}\ 0\le z\le 6\,. \tag{5}$$

Cylindrical segments of radius R_{in} for $-2<z<0$, and of radius $2R_{\text{in}}$ for $6<z<8$ are added upstream and downstream the diffuser. The inlet radius is taken $R_{\text{in}}=\sqrt{2}$.

The inlet swirl corresponds to a Burgers vortex, with velocity components given by

$$V_{z\,\mathrm{in}} = 1;\; V_{r\,\mathrm{in}} = 0;\; V_{\theta\,\mathrm{in}}(r) = \frac{\Omega R^2}{r}\left[1 - \exp\left(-\frac{r^2}{R^2}\right)\right], \tag{6}$$

where Ω is the angular velocity at the axis, and R is the vortex characteristic radius. Note that the asymptotic behavior of the swirl velocity is

$$V_\theta \approx \Omega R \frac{r}{R} \text{ if } r \ll R, \text{ and } V_\theta \approx \Omega R \frac{R}{r} \text{ if } r \gg R, \tag{7}$$

corresponding to the forced vortex (rigid body rotation) and free vortex, respectively. The characteristic radius is taken $R=0.4$, constant for all numerical experiments, but the swirl intensity is increased as $\xi \equiv 2\Omega R_{\mathrm{in}} / V_{z\,\mathrm{in}} = 1$, 2, and 3. The outlet conditions for unsteady flow simulations should meet the basic requirement of recovering the correct solution in a truncated domain, without spurious reflections that artificially contaminate the flow field. Jin and Braza (Ref 9) develop nonreflecting outlet boundary conditions for unsteady Navier-Stokes calculations and test them successfully for the onset of instability and the development of organized structures in 2D free shear layer flows. The dynamical characteristics of the flow, such as the roll-up process, the growth of mixing layer, and the predominant frequency are correctly predicted. Paik et al. (Ref 10) develop and implement non-reflecting characteristic-based outlet boundary conditions, and use them in a full 3D unsteady turbulent flow simulation in a turbine draft tube. In our present computations we have used a simple radial pressure equilibrium condition on the outflow section,

$$\frac{\partial p}{\partial r} = \frac{\rho V_\theta^2}{r}, \tag{8}$$

derived from the radial projection of the momentum equation (3) for vanishing radial velocity. Although this condition is valid for both steady and unsteady fully developed flows, its accuracy deteriorates when a vortex ring is convected downstream through the outlet section. However, our main concern is not focused on the accuracy of unsteady flow simulations. Instead, we are primarily interested in identifying the main features of the unsteady flow, and more important in recovering a steady axisymmetric flow using an axial jet to control the flow.

Figure 1 shows the streamlines in a meridional half-plane for a low swirl intensity, $\xi=1$, when the flow is steady and no vortex breakdown occurs. The axial velocity profiles at inlet and outlet show a quasi-uniform flow deceleration, while outlet swirl velocity is obviously decaying according to Kelvin's theorem $rV_\theta=constant$ along streamlines. As the swirl intensity increases to $\xi=2$, a steady axisymmetric vortex breakdown occurs at the end of the diffuser, with the development of a central stagnation region, Fig. 2. Such solutions have been obtained by Keller et al. (Ref 2) for Rankine vortices as well, using the Long-Squire equation. In our case, the solution is obtained by solving the unsteady axisymmetric Euler equations in primary variables, by setting a vanishing recirculation velocity on the outlet section. The stagnation region is also clearly identified in the axial and swirl velocity profiles on the outlet section.

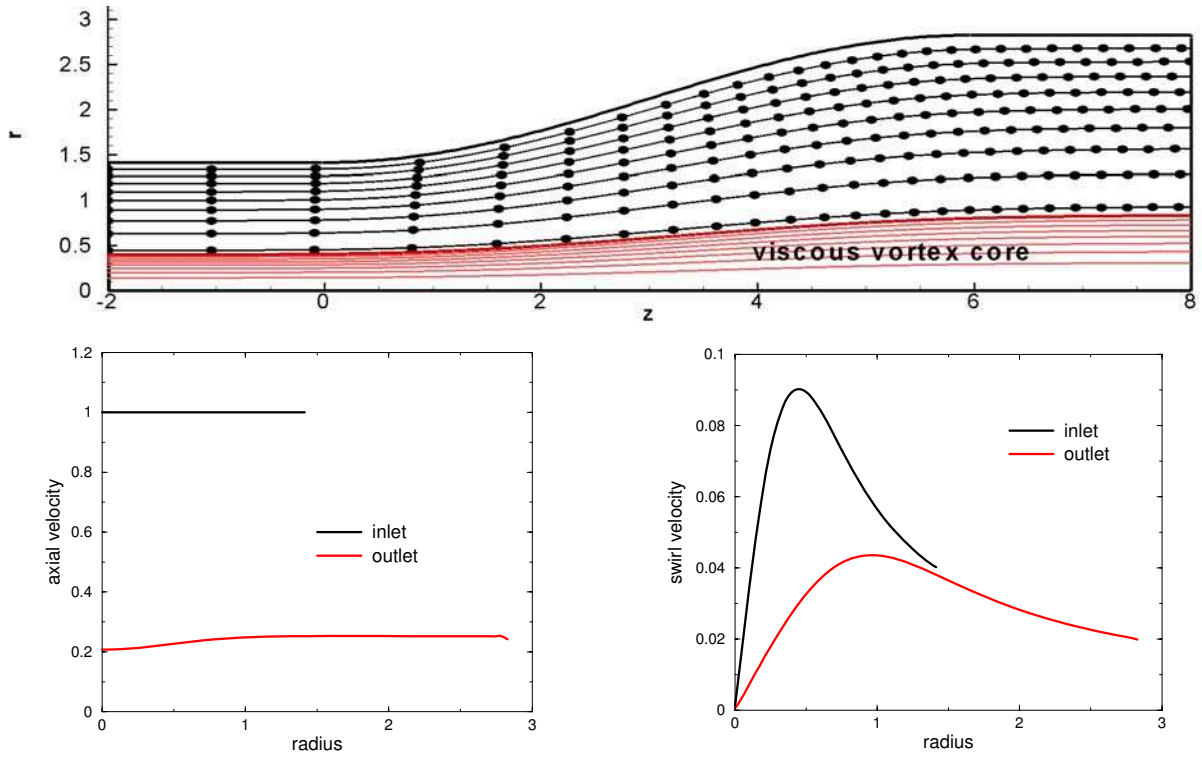

Figure 1. Steady swirling flow without vortex breakdown for $2\Omega R_{\text{in}} / V_{z\,\text{in}} = 1$**.**

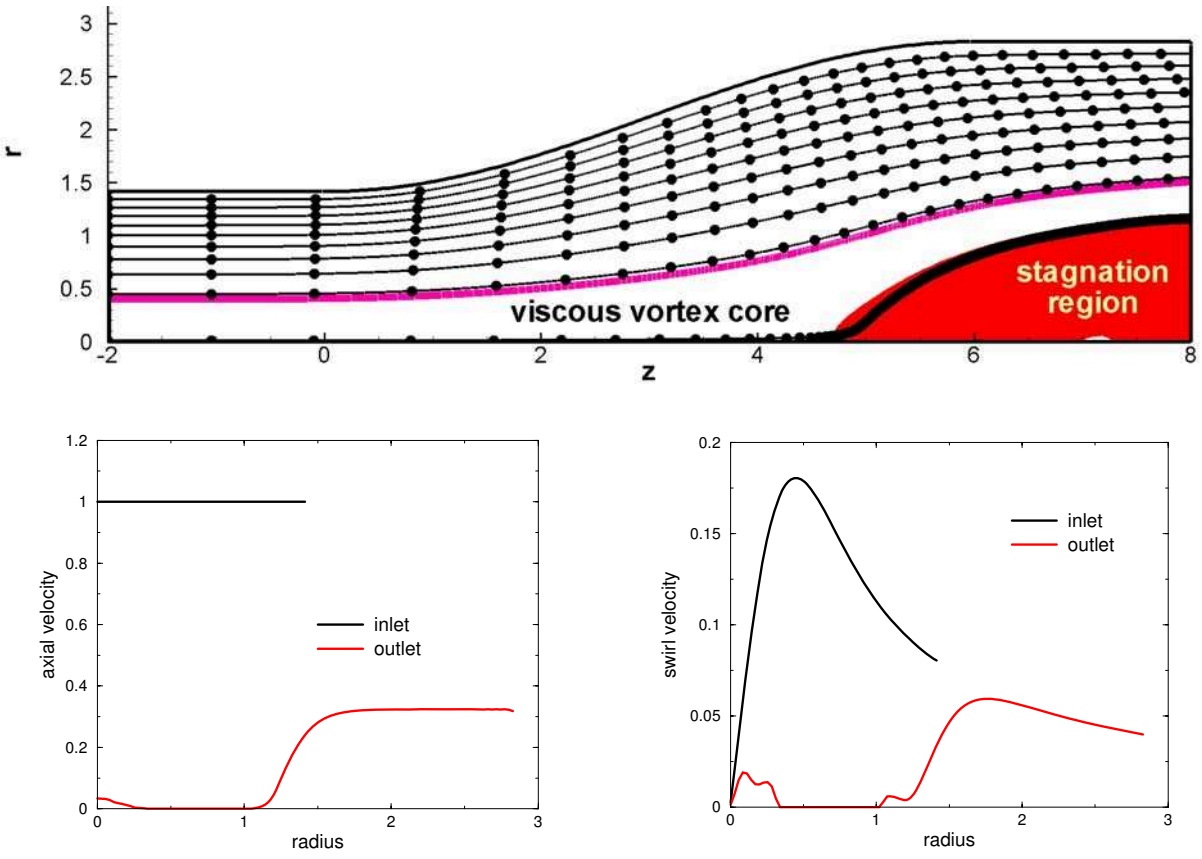

Figure 2. Steady vortex breakdown with central stagnation region for $2\Omega R_{\text{in}} / V_{z\,\text{in}} = 2$**.**

Usually, when the flow presents a recirculation on the outlet section, on this region the fluid from downstream (re)enters into the computational domain and the velocity vector, as well as turbulence quantities when turbulent flow is considered, must be specified. Mathematical, as well as physical, arguments led Goldshtik and Hussain (Ref 11) to advocate once more for the flow model with stagnant separation zones while analyzing the inviscid vortex breakdown in a semi-infinite pipe. It is this model we recognize in Fig. 2, as the result of an unsteady axisymmetric Euler simulation with vanishing recirculation on outlet. The time markers on the streamlines from Figures 1 and 2 show the flow deceleration in the meridional half plane. For example, the streamline originating close to the axis in Fig. 2 displays a severe flow deceleration as the fluid particles approach the tip of the stagnation region, then the velocity practically vanishes. The streamline originating at the vortex characteristic radius on the inlet section, which conventionally separates the inner so-called viscous core from the outer inviscid-like flow, is shown in thick red solid line.

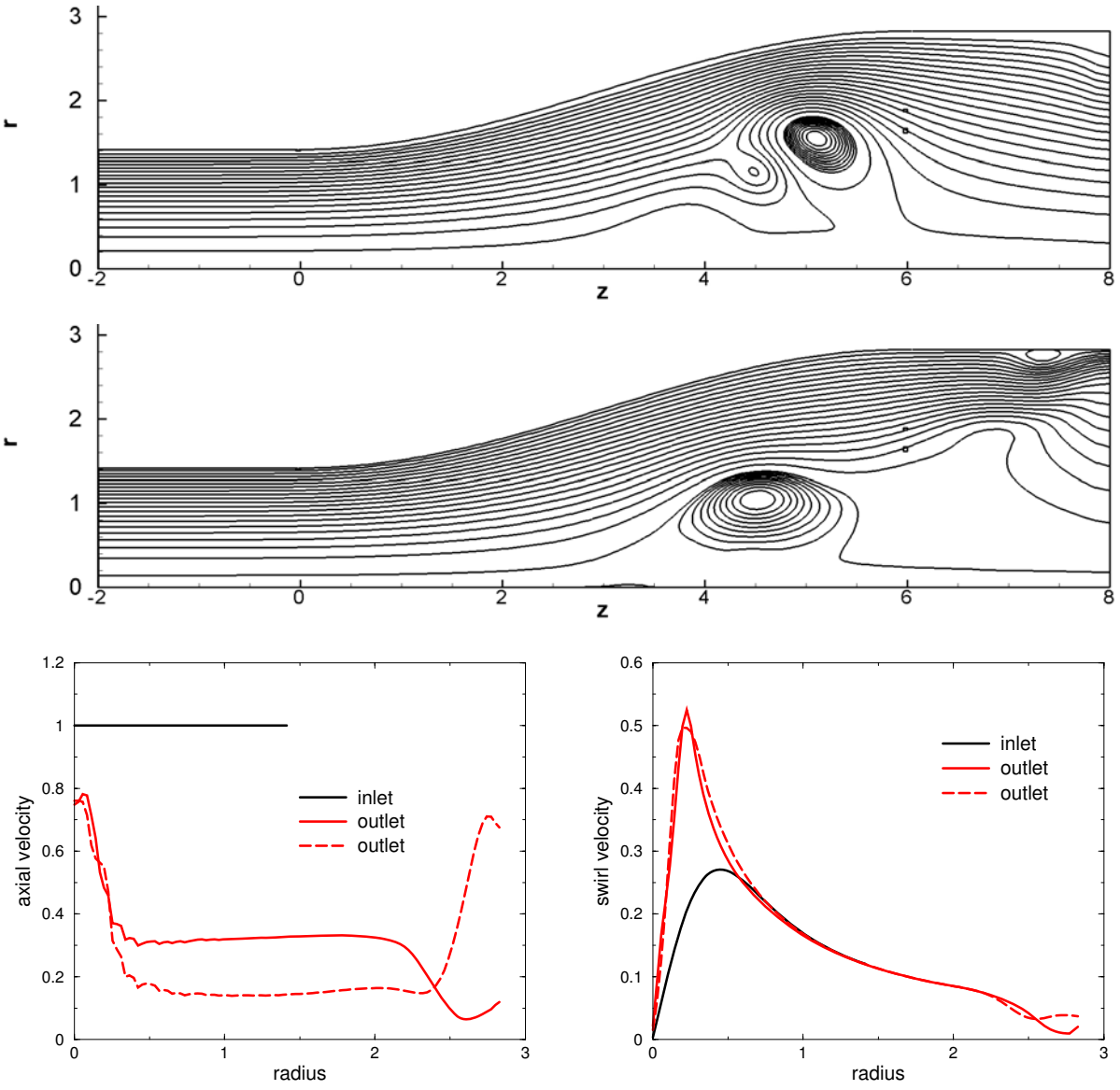

Figure 3 Unsteady swirling flow for $2\Omega R_{\text{in}} / V_{z\,\text{in}} = 3$ at two instants in time.

When the swirl intensity is further increased, $\xi=3$, the flow configuration changes dramatically. Instead of obtaining a steady configuration with a larger central stagnation region, the flow becomes highly unsteady, with periodic vortex rings development and convection downstream. Figure 3 shows two snapshots of the streamlines in the meridional half plane, with distinct vortex rings. Moreover, the radial discharge distribution on the outlet section is shifting significantly in time, leading to pressure fluctuations. Although the inviscid steady swirling flows are loss-free, as shown by the numerical experiments, the energy balance for unsteady flow show that a fraction of the overall kinetic energy is trapped within the vortex rings. The dimensionless specific energy deficit,

$$\Delta E = \frac{\frac{1}{Q}\left[\int_{S_{\text{in}}}\left(\frac{p}{\rho}+\frac{V^2}{2}\right)\vec{V}\cdot\vec{n}\,dS - \int_{S_{\text{out}}}\left(\frac{p}{\rho}+\frac{V^2}{2}\right)\vec{V}\cdot\vec{n}\,dS\right]}{Q^2/2A_{\text{in}}^2}, \tag{9}$$

is plotted in Fig. 4 against the time. One can easily see that during the vortex ring development within the computational domain the average specific energy at the inlet is significantly larger than the corresponding value at the outlet due to the kinetic energy accumulating within the growing vortex ring. However, when the vortex ring is convected through the outlet section, a burst of specific energy can be observed. The phenomenon is not quite periodic, most likely due to the simple outlet condition that is not exactly non-reflecting.

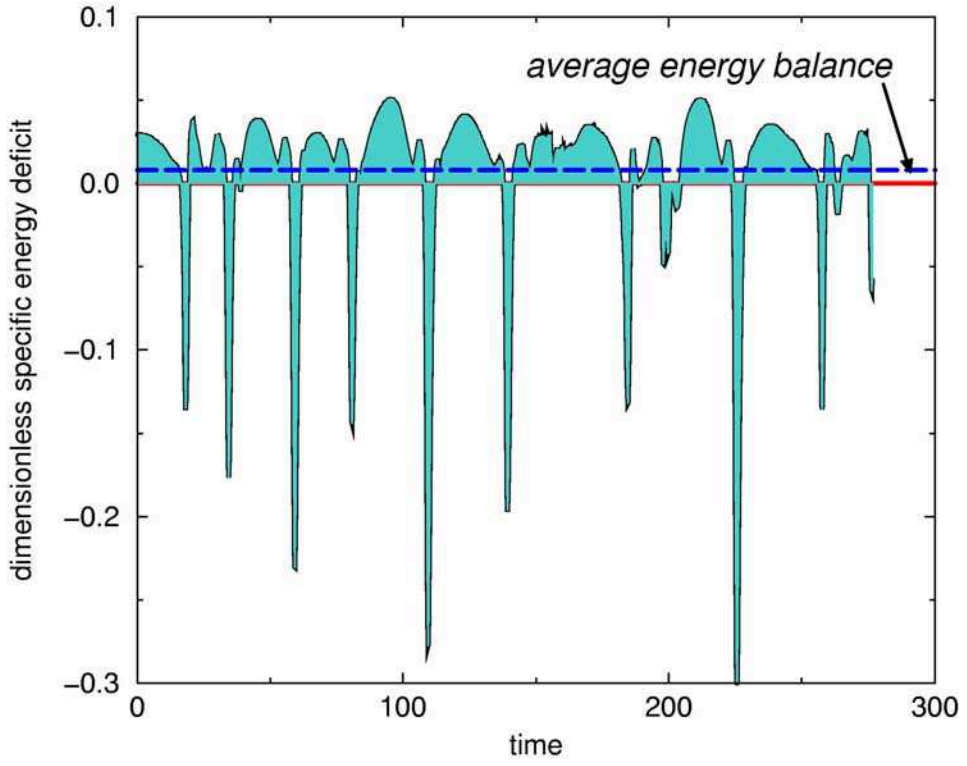

Figure 4. Inlet-outlet specific energy imbalance for unsteady swirling flow.

Let us introduce a small perturbation in the inlet axial velocity profile, in the form of a jet at the axis,

$$V_{z\,\mathrm{in}}(r) = 1 + U_{\mathrm{jet}} \exp\left(-\frac{r^2}{R_{\mathrm{jet}}^2}\right), \tag{10}$$

where U_{jet} is the jet amplitude and R_{jet} is the jet characteristic radius. The exponential velocity profile is characteristic to submerged jets. When introducing the modified inlet axial velocity (10), with U_{jet}=0.5 and R_{jet}=0.1 R_{in}, for the swirl intensity ξ=*3*, the flow recovers a steady configuration with complete removal of the vortex rings, as shown in Fig. 5. Note that the additional jet discharge is $Q_{\mathrm{jet}} = U_{\mathrm{jet}} \pi R_{\mathrm{jet}}^2$, i.e. 0.5% of the initial discharge corresponding to a constant inlet axial velocity. The axial velocity at outlet marginally approaches an annular quasi-stagnation region, and the swirl velocity displays a significant decay with respect to the inlet swirl.

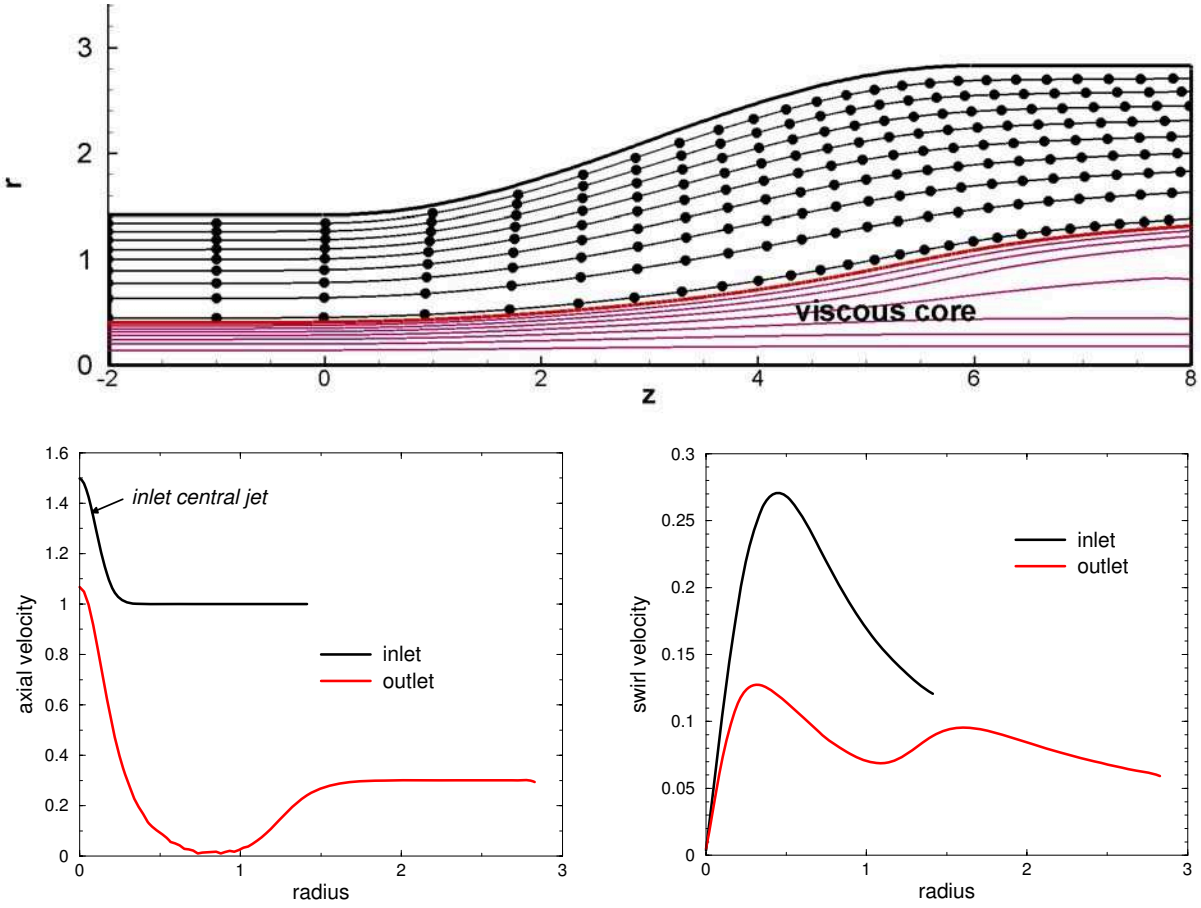

Figure 5. Swirling flow at $2\Omega R_{\mathrm{in}} / V_{z\,\mathrm{in}} = 3$ stabilized with inlet central jet.

The important result shown in Fig. 5 proves that the unsteady swirling flows can be controlled with the injection of a central jet. This idea follows the conclusion of Zhang et al. (Ref 5) that the axial-flow velocity profile on the inlet plays a key role in the absolute/convective instability character of the swirling flow in the cone of a Francis turbine draft tube. In the case of Francis turbines this jet would be injected through the hollow runner shaft, being supplied with high pressure water from upstream the turbine. Moreover, since no kinetic energy is trapped within the unsteady vortex rings hydraulic losses will diminish significantly.

Axisymmetric turbulent flow in the draft tube cone of a Francis turbine

The velocity field downstream the runner of a Francis turbine scaled model of specific speed 0.56 has been investigated experimentally (Ref 12) within the FLINDT project (Ref 8). We have shown in (Ref 4) that the experimental data for both axial and swirl velocity profiles measured on a survey section S1 at the beginning of the draft tube cone can be accurately represented by a system of three vortices:

$$V_z(r) = U_0 + U_1 \exp\left(-r^2/R_1^2\right) + U_2 \exp(-r^2/R_2^2), \tag{11a}$$

$$V_\theta(r) = \Omega_0 r + \Omega_1 \frac{R_1^2}{r}\left[1 - \exp\left(-\frac{r^2}{R_1^2}\right)\right] + \Omega_2 \frac{R_2^2}{r}\left[1 - \exp\left(-\frac{r^2}{R_2^2}\right)\right] \tag{11b}$$

The *Vortex0* is a rigid body rotation with angular speed Ω_0 and a constant axial velocity U_0. *Vortex1*, which has a vortex core extent R_1 about half the wall radius, is counter-rotating and co-flowing with respect to *Vortex0*. The strength of this vortex, both in Ω_1 as well as in U_1 is growing as the flow rate increases. *Vortex2* has a core at least four times smaller than *Vortex1*, is co-rotating and counter-flowing with respect to *Vortex0*, and its strength increases as the flowrate decreases. The dashed lines in Figs. 6a and 6b show the least squares fit with Eqs. 10 of the measured velocity profiles (circles) at four operating points, but in (Ref 4) we have checked this analytical representation at 17 operating points around BEP, in excellent agreement with experimental data for both axial and swirl velocity profiles. Our analysis has shown that *Vortex2* can be associated with the runner crown wake, where the specific energy deficit is growing as the discharge decreases. The velocity field was also measured in a survey section S2, further downstream in the draft tube cone, with the results shown as square points in Figs. 6a and 6b. These measurements are used here to validate and to assess the accuracy of the axisymmetric turbulent flow solver from FLUENT 6.2.16.

The numerical results of our numerical simulations, shown with solid lines in Figs. 6a and 6b, were obtained in a computational domain corresponding to the cone with 8.5° angle extended downstream with a cylindrical part. Besides the axial and swirl velocity profiles, we have specified at the inlet the turbulent quantities for the $k-\varepsilon$ model. The turbulent kinetic energy k is available from experiments, and the dissipation rate is evaluated as $\varepsilon = C_\mu^{3/4} k^{3/2} / L_\varepsilon$, where $C_\mu = 0.09$ and the turbulence length scale is taken $L_\varepsilon = 0.02 R_{\text{in}}$ to match the experimental data at all operating points.

Four operating points are investigated in this paper, within ±10% the best efficiency discharge Q_{BEP}. The corresponding discharge coefficient, $\varphi \equiv Q/\omega R_{ref} A_{ref}$, with ω the runner angular speed, R_{ref} and A_{ref} the runner outlet radius and area, respectively, ranges from 0.34 to 0.41.

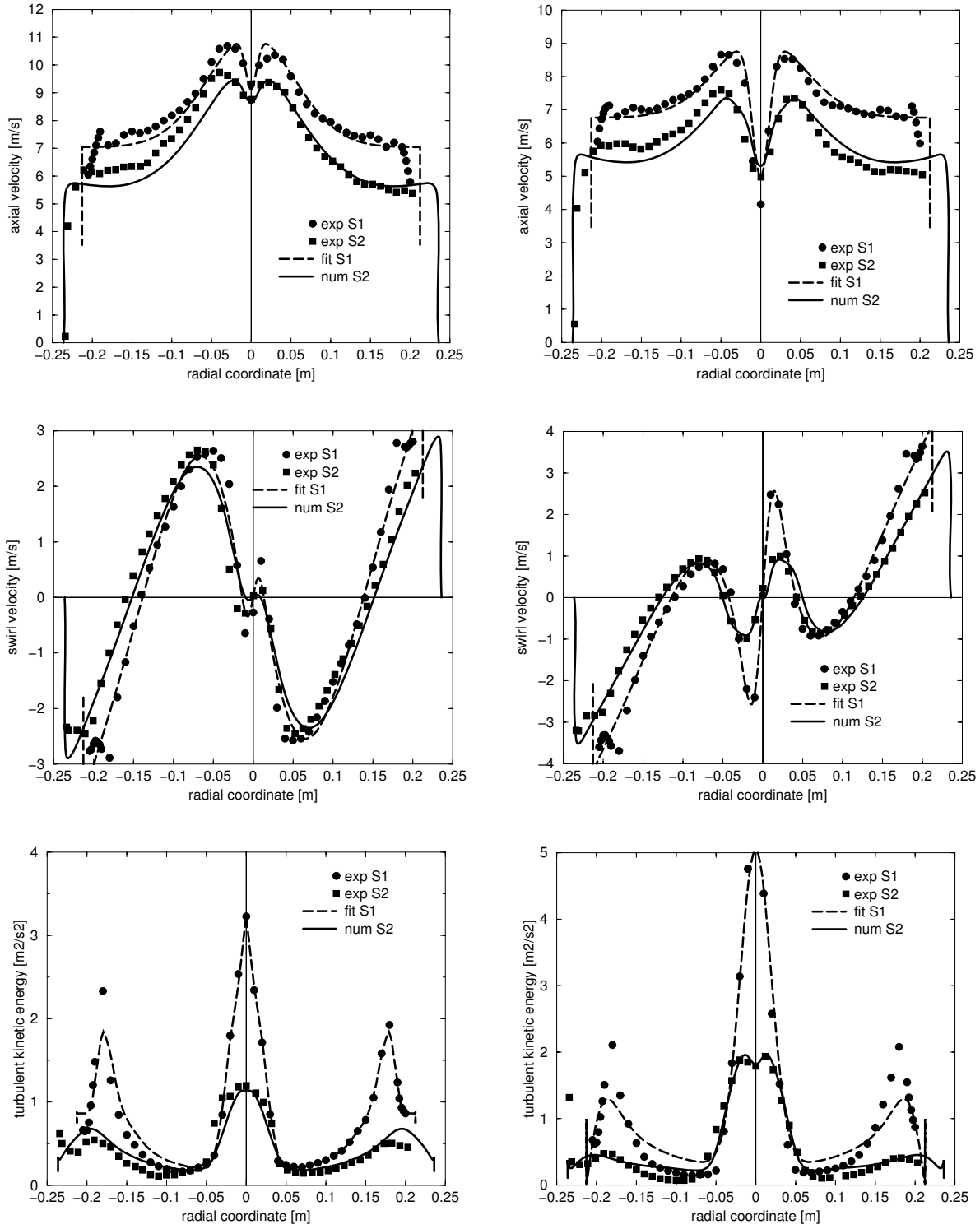

$\varphi = 0.410$ $\varphi = 0.380$

Figure 6a. Velocity and turbulent kinetic energy profiles at $1.11 \times Q_{BEP}$ and $1.03 \times Q_{BEP}$.

One can see that for discharge larger or equal to the Q_{BEP} the axial and swirl velocity profiles, as well as the turbulence decay, are very well predicted in the survey section S2. At part discharge the axial and circumferential velocity profiles are still in excellent agreement with experiemental data, while the turbulence decay slightly departs from experiment near

centerline. In this case, the inlet flow itself has an axial velocity profile that practically goes to zero at the axis, while in the central region the turbulent kinetic energy is quite large. This indicates strong central velocity fluctuations with a vanishing mean value, which may be the result of a coherent unsteady flow structure (e.g. a weak helical vortex) rather than a genuine turbulent flow. The conclusion is that for partial discharge flow simulations in the turbine draft tube cone, instead of imposing velocity profiles at a cross section downstream the runner a full unsteady flow calculation that includes the runner must be considered.

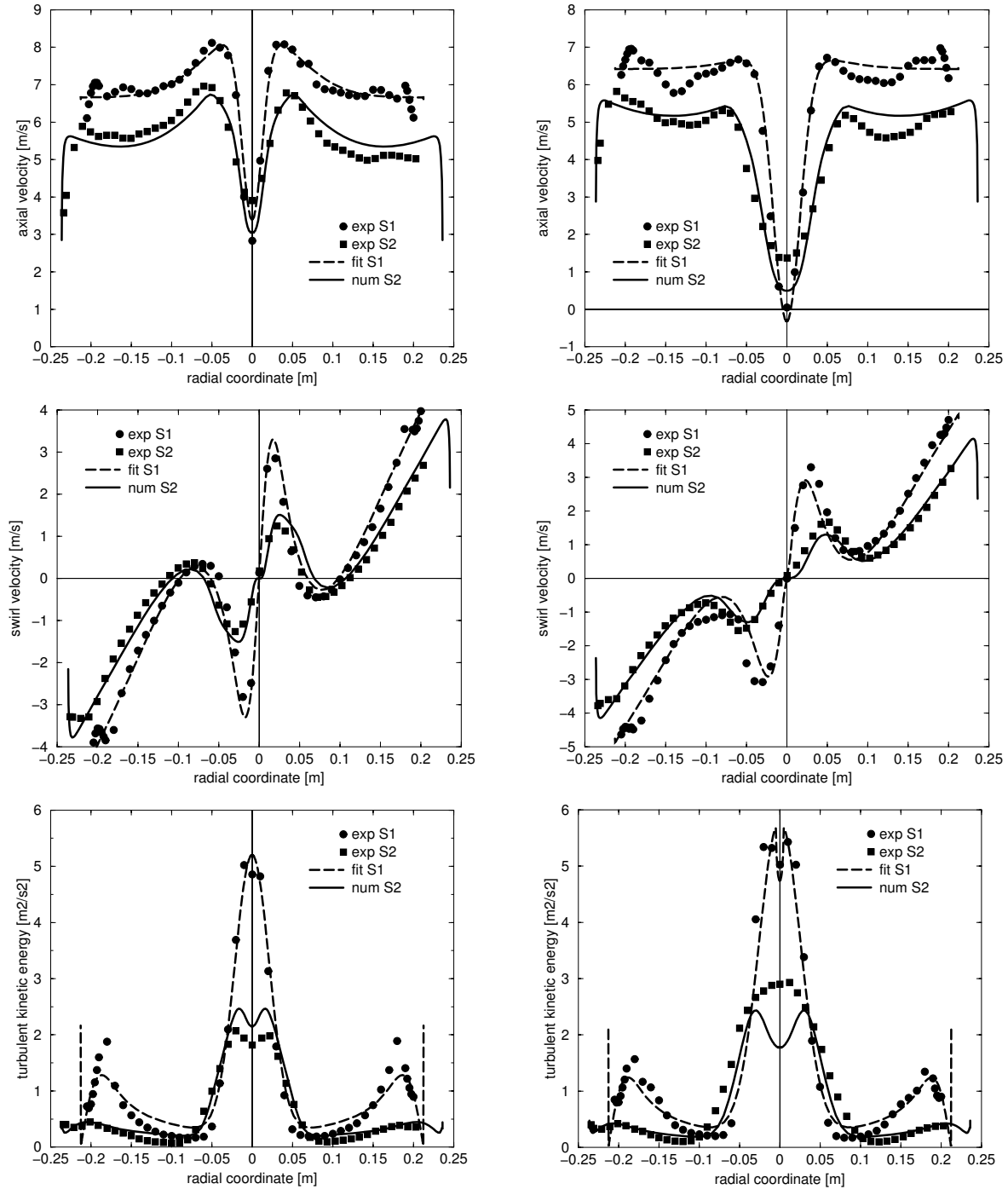

$\varphi = 0.368$ $\varphi = 0.340$

Figure 6b. Velocity and turbulent kinetic energy profiles at Q_{BEP} and $0.92 \times Q_{BEP}$.

An important ingredient for the success of the present numerical simulations is the Reynolds stress model (RSM) which computes the individual Reynolds stresses using differential transport equations. The individual Reynolds stresses are then used to obtain closure of the Reynolds-averaged momentum equation. RSM is known to perform better than the k-ε model in turbulent swirling flows, and the results above confirm that it can capture the physical mechanisms of the turbulent mixing of the blade-to-blade shear flow investigated experimentally by Iliescu et al. (Ref 13) in the draft tube cone of the FLINDT Francis turbine.

Conclusions

The paper investigates numerically decelerated swirling flows, using both inviscid and viscous axi-symmetric flow models. The evolution of a Burgers vortex in a sinusoidal diffuser is investigated using the FLUENT unsteady axi-symmetric Euler solver, for three values of inlet swirl intensity. The first case results in a steady axi-symmetric configuration with a quasi-uniform deceleration of the flow up to the outlet section. The second case, with a larger inlet swirl, displays a strong axial flow deceleration and the development of a stagnant central region. This is a typical case of axisymmetric vortex breakdown. The unsteady flow solver also converges into a steady stable configuration. By further increasing the inlet swirl intensity the flow becomes unsteady, with periodic vortex rings generation and convection downstream. Through the inlet/outlet energy balance we show that a significant fraction of kinetic energy is trapped inside the vortex rings. Such flows cannot be covered by the steady axi-symmetric inviscid flow model that reduces to the Long-Squire equation for the Stokes streamfunction. However, this is the case for the swirling flows downstream the Francis runners when the turbine operates at part discharge.

Our main result shows that a small alteration of the inlet axial velocity profile, by injecting a weak axial jet with only 0.5% from the overall discharge, is able to bring the unsteady swirling flow from the third case back to a steady unidirectional flow configuration. This novel flow control technique is particularly suited for Francis turbine, where an axial jet can be easily supplied with high pressure water from upstream the spiral case through the tubular shaft. The hydraulic energy corresponding to the jet discharge could be fully compensated by the decrease of hydraulic losses due to the unsteady vortices dissipation. In addition, the severe pressure fluctuations associated with flow unsteadiness at part load are practically eliminated.

Further investigations on the swirling flow control technique should rely on turbulent flow simulations. This is why we have investigated the accuracy of the axi-symmetric turbulent flow solver from the FLUENT code using experimental data for velocity and turbulent kinetic energy on two survey sections in the draft tube cone of a model Francis turbine. By imposing the velocity and turbulent kinetic energy profiles on the upstream survey section as inlet conditions, we compute the corresponding quantities on the downstream survey section. It is shown that both axial and swirl velocity profiles, as well as the turbulent kinetic energy decay, are very well predicted in comparison with experimental data. This is largely due to the Reynolds stress model employed in our computations, which is known to perform better than

other turbulence model in highly anisotropic swirling flows. Moreover, particular attention has been devoted to the turbulence specification on the inlet section, where a correct turbulent length scale has been chosen to compute the inlet turbulent dissipation rate.

Acknowledgements

The present research is supported from the Joint Research Project IB7320-110942/1 funded by the Swiss National Science Foundation within the programme "Scientific Co-operation between Eastern Europe and Switzerland" (SCOPES), as well as by the Romanian National University Research Council (CNCSIS) under consortium grant No. 33.

References

Ref 1 Zangeneh, M., "A compressible three-dimensional design method for radial and mixed flow turbomachinery blades", Int. J. Numerical Methods in Fluids, Vol. 13, pp. 599-624, 1991.

Ref 2 Keller, J.J., Egli, W., and Althaus, R., "Vortex breakdown as a fundamental element of vortex dynamics", Journal of Applied Mathematics and Physics (ZAMP), Vol. 39, pp. 404-440, 1988.

Ref 3 Benjamin, T.J., "Theory of the Vortex Breakdown Phenomenon", J. Fluid Mechanics, Vol. 14, pp. 593-629, 1962.

Ref 4 Susan-Resiga, R., Ciocan, G.D., Anton, I., and Avellan, F., "Analysis of the swirling flow downstream a Francis turbine runner", Journal of Fluids Engineering, Vol. 128, pp. 177-189, 2006.

Ref 5 Zhang, R.-K., Cai, Q.-D., Wu, J.-Z., Wu, Y.-L., Liu, S.-H., and Zhang, L., "The Physical Origin of Severe Low-Frequency Pressure Fluctuations in Giant Francis Turbines", Modern Physics Letters B, Vol. 19, Issue 28-29, pp. 1527-1530, 2005.

Ref 6 Gallaire, F., Ruith, M., Meiburg, E., Chomaz, J.-M., and Huerre, P., "Spiral vortex breakdown as a global mode", Journal of Fluid Mechanics, Vol. 549, pp. 71-80, 2006.

Ref 7 Darmofal, D.L., "Comparisons of Experimental and Numerical Results for Axisymmetric Vortex Breakdown in Pipes", Computers & Fluids, Vol. 25, No. 4, pp. 353-371, 1996.

Ref 8 Avellan, F., "Flow Investigation in a Francis Draft Tube: The FLINDT Project", Proceedings of the 20th IAHR Symposium on Hydraulic Machinery and Systems, Paper DES-11, 2000.

Ref 9 Jin, G., and Braza, M., "A Nonreflecting Outlet Boundary Condition for Incompressible Unsteady Navier-Stokes Calculations", Journal of Computational Physics, Vol. 107, pp. 239-253, 1993.

Ref 10 Paik, J., Sotiropoulos, F., and Sale, M.J., "Numerical Simulation of Swirling Flow in a Complex Hydroturbine Draft Tube using Unsteady Statistical Turbulence Models", Journal of Hydraulic Engineering, Vol. 131, Issue 6, pp. 441-456, 2005.

Ref 11 Goldshtik, M. and Hussain, F., "Analysis of inviscid vortex breakdown in a semi-infinite pipe", Fluid Dynamics Research, Vol. 23, pp. 189-234, 1998.

Ref 12 Ciocan, G.D., and Avellan, F., "Flow Investigations in a Francis Draft Tube: Advanced Experimental Methods", Proc. 3rd Conference of Romanian Hydropower Engineers, Bucharest, Romania, 2004.

Ref 13 Iliescu, M.S., Ciocan, G.D., Avellan, F., "Experimental Study of the Runner Blade-to-Blade Shear Flow Turbulent Mixing in the Cone of Francis Turbine Scale Model", Proc. 22nd IAHR Symposium on Hydraulic Machinery and Systems, Stockholm, Sweden, 2004.